ECS Journal of Solid State
Science and Technology

The Electrochemical Society
Advancing solid state & electrochemical science & technology

OPEN ACCESS

Origin of Voids at the SiO_2/SiO_2 and SiCN/SiCN Bonding Interface Using Positron Annihilation Spectroscopy and Electron Spin Resonance

To cite this article: F. Nagano *et al* 2023 *ECS J. Solid State Sci. Technol.* **12** 033002

View the article online for updates and enhancements.

You may also like

- A Comparative Study of SiCN_Si and SiCN_SiCN Junctions for High-Temperature Ultraviolet Detecting Applications
Tse-Heng Chou, Yean-Kuen Fang, Che-Yun Yang et al.
- Progress in polymer-derived functional silicon-based ceramic composites for biomedical and engineering applications
A Francis
- Selective Polishing of Amorphous Silicon Carbonitride (a-SiCN) Films Over Silicon Dioxide and Silicon Nitride Films for Hardmask Applications
Akshay Gowda, Sridevi Alety, Charith K. Ranaweera et al.

Investigate your battery materials under defined force!
The new PAT-Cell-Force, especially suitable for solid-state electrolytes!

- Battery test cell for force adjustment and measurement, 0 to 1500 Newton (0-5.9 MPa at 18mm electrode diameter)
- Additional monitoring of gas pressure and temperature

www.el-cell.com +49 (0) 40 79012 737 sales@el-cell.com

EL-CELL®
electrochemical test equipment

This content was downloaded from IP address 87.64.20.8 on 24/05/2023 at 11:58

ECS Journal of Solid State Science and Technology, 2023 **12** 033002

Origin of Voids at the SiO_2/SiO_2 and SiCN/SiCN Bonding Interface Using Positron Annihilation Spectroscopy and Electron Spin Resonance

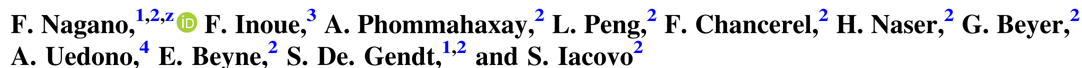

F. Nagano,[1,2,z] F. Inoue,[3] A. Phommahaxay,[2] L. Peng,[2] F. Chancerel,[2] H. Naser,[2] G. Beyer,[2] A. Uedono,[4] E. Beyne,[2] S. De. Gendt,[1,2] and S. Iacovo[2]

[1]*Department of Chemistry, KU Leuven, Celestijnenlaan 200f, 3001 Leuven, Belgium*
[2]*imec, Kapeldreef 75, 3001 Leuven, Belgium*
[3]*Faculty of Engineering, Yokohama National University, 79-5 Tokiwadai, Hodogaya, Yokohama 240-8501, Japan*
[4]*Faculty of Pure and Applied Science, University of Tsukuba, Tsukuba, Ibaraki 305-8573, Japan*

To obtain reliable 3D stacking, a void-free bonding interface should be obtained during wafer-to-wafer direct bonding. Historically, SiO_2 is the most studied dielectric layer for direct bonding applications, and it is reported to form voids at the interface. Recently, SiCN has raised as a new candidate for bonding layer. Further understanding of the mechanism behind void formation at the interface would allow to avoid bonding voids on different dielectrics. In this study, the void formation at the bonding interface was studied for a wafer pair of SiO_2 and SiCN deposited by plasma enhanced chemical vapor deposition (PECVD). The presence of voids for SiO_2 was confirmed after the post-bond anneal (PBA) at 350 °C by Scanning Acoustic Microscopy. Alternatively, SiCN deposited by PECVD has demonstrated a void-free interface after post bond annealing. To better understand the mechanism of void formation at the SiO_2 bonding interface, we used Positron Annihilation Spectroscopy (PAS) to inspect the atomic-level open spaces and Electron Spin Resonance (ESR) to evaluate the dangling bond formation by N_2 plasma activation. By correlating these results with previous results, a model for void formation mechanism at the SiO_2 and the absence of for SiCN bonding interface is proposed.
© 2023 The Author(s). Published on behalf of The Electrochemical Society by IOP Publishing Limited. This is an open access article distributed under the terms of the Creative Commons Attribution 4.0 License (CC BY, http://creativecommons.org/licenses/by/4.0/), which permits unrestricted reuse of the work in any medium, provided the original work is properly cited. [DOI: 10.1149/2162-8777/acbe18]

Manuscript submitted December 27, 2022; revised manuscript received February 7, 2023. Published March 2, 2023.

Supplementary material for this article is available online

Recently, the downsizing of integrated circuits (ICs) in a planar concept, is becoming challenging due to physics' limitations of the lithography process. The further development of 2D scaling and its mass production are incredibly expensive nowadays. Due to this high cost of development and production, the performance of semiconductor devices is not following anymore the growth curve that Moore advocated in his so-called Moore's law if we pursue the 2D scaling only.[1] To overcome the challenging assignment of 2D down scaling, 3D integration techniques for ICs have shown promise in making it an alternative solution. By integrating the ICs in a vertical direction, the density of components per area can be increased. Furthermore, 3D integration also helps in enriching the device's functionality and power efficiency by stacking CMOS on the top of application-specific integrated circuit (ASIC), and back-side power delivery network (BSPDN).[2,3] In the 3D integration schemes, direct bonding is an attractive integration concept that does not use any adhesives between the structures to be bonded. In this approach the exposed Cu pads surface and neighboring dielectric layer are bonded onto another patterned surface allowing connection between Cu pads, such a process is called Hybrid bonding. The direct bonding has been mainly attempted on wafer level and die level stacking in general in semiconductor field. Wafer-to-wafer direct bonding provides some advantages such as high bonding accuracy, stability, and throughput. The mechanical stability and uniformity of bonded wafer pairs is governed by the direct bonding interface of the dielectric layers since the approximately 75% of patterned surface is occupied by a dielectric layer. To guarantee the mechanical performance of wafer-to-wafer direct bonding, uniform and strong bonding of dielectric layers is essential. Therefore, the fundamental understanding of the direct bonding of dielectric layers is required.

SiO_2 is a well-studied dielectric layer for the direct bonding, but several researchers have reported that SiO_2 shows limited performance for direct bonding because of lower bonding strength and air bubble formation.[4,5] This void formation occurs primarily after the post-bond anneal process at elevated temperature over 350 °C, resulting in electrical yield loss of the 3D IC.

Silicon carbon nitride, SiCN, has been developed as an alternative bonding material for the direct bonding.[6,7] It has been demonstrated that SiCN obtained a higher bonding strength – 2.5 J m^{-2} equivalent to Si bulk strength. Moreover, although a SiCN bonded wafer pair was annealed at a higher temperature of 450 °C, SiCN does not appear to form any voids at the bonding interface.[6,7] However, up to now, limited fundamental understanding for the SiCN bonding mechanism has been developed. In addition, although several researchers have proposed that the origin of the void formation of SiO_2 relates to the presence of water, its appearance at the surface and at the interface has not been studied. In this study, to clarify the origin of void formation induced during the post-bond annealing, atomic-level defects were analyzed using positron annihilation spectroscopy (PAS) for SiCN and SiO_2 layer. This analytical technique can be used for the evaluation of the open space in amorphous material and vacancy type defects in (semiconductor) materials.[8] Furthermore, past work has suggested that not only the hydrophilicity of the surface but also dangling bonds contribute to the direct bonding of SiCN. Moreover, the dangling bond is also expected to be related to the void formation at PBA during the direct bonding. Therefore, in this study the dangling bonds density on the surface of SiO_2 and SiCN before and after surface plasma treatment is inspected using Electron Spin Resonance (ESR). The aim of this article is to propose a model for the void formation mechanism during the post-bond annealing of SiO_2 layers and to explain the suppression effect of void formation of SiCN layer through the observation of PAS and ESR measurements. The characterization methodology will be presented in detail in the following sections.

Experimental

Sample preparation.—Different dielectrics layers on Si have been prepared to be inspected using different techniques described in detail in the following paragraphs. In all the cases 300 mm p-type Si

[z]E-mail: Fuya.Nagano@imec.be

Table I. Thickness and roughness of SiO_2 and SiCN films after each process.

	Thickness, nm		Roughness, R_a, nm	
	After PECVD	After CMP	After PECVD	After CMP
SiO_2	123.9 ± 1.9	92.4 ± 3.4	0.79	0.20
SiCN	120.9 ± 1.4	94.1 ± 1.7	0.40	0.09

(100) wafers were used. Either SiO_2 or SiCN dielectric layers were deposited by plasma enhanced chemical vapor deposition (PECVD) at 370 °C. Deposition precursors are NH_3 and $SiH_x(CH)_y$ for SiCN, and SiH_4 and N_2O for SiO_2. Table I shows the summary of the measured thickness and the arithmetic average of the roughness profile, R_a, after PECVD and CMP for the SiO_2 and SiCN films. The thickness of a dielectric layer was targeted 120 nm and a control measurement by Spectroscopic Ellipsometry (F5-SCD, KLA-Tencor) was done. After the PECVD process, wafers were exposed to a post-depo anneal (PDA) process at 400 °C for 10 min in 10% H_2/N_2 ambient in a furnace (A412, ASM) to evacuate precursor residues, impurities, and moisture inside. After the PDA process, all wafers were planarized and smoothened by a CMP process with optimized slurry and polish pad. The dielectric thickness of SiO_2 and SiCN was measured as 92 nm and 94 nm after the CMP process. The arithmetic average of the roughness profile, R_a, after CMP, was determined from a scan field of 500 nm × 500 nm by atomic force microscope (AFM, NX3DM, Park Systems). The obtained smoothened dielectric surfaces show $R_a$in the sub-nano meter range with values of 0.20 nm for SiO_2 and 0.09 nm for SiCN.

After the CMP process, one wafer of each kind (SiO_2 and SiCN) was diced to 20 × 20 mm^2 pieces, and these diced samples were characterized with ESR measurement to measure the dangling bond density before N_2 plasma activation. Other SiO_2 and SiCN wafers were activated by a N_2 plasma activation process in the EVG GEMINI wafer bonding tool. After the surface activation process, a deionized water rinse of the surface is applied to remove the CMP particles on the surface. To investigate the OH group density on the surface of the dielectrics the samples were prepared in the following way. One SiO_2 and one SiCN wafer that received N_2 plasma activation was diced to 20 × 20 mm^2 pieces. On some of these diced samples we applied 1 cycle of $HfCl_4$ deposition and subjected them to Rutherford Back-Scattering Spectroscopy (RBS) to measure the Hf thickness to study the OH concentration on the surface.[9] Moreover, some other samples diced from single wafer received N_2 plasma were subjected to the ESR measurement to inspect the dangling bonds of SiO_2 and SiCN layer after N_2 plasma activation.

The remaining wafers were then bonded together, with identical top and bottom wafers for both the SiO_2 and SiCN. Bonding was performed using EVG GEMINI system performing N_2 plasma activation, water rinsing prior to bonding. After room temperature bonding, the bonding uniformity and presence of voids at the bonding interface on the whole 300 mm wafer pair was verified by in-line scanning acoustic microscopy (SAM, AW-SAM300, PVA Tepla). The bonded wafers were then taken through a post-bond anneal (PBA) process at a temperature of 250 °C for 2 h under N_2 ambient in a furnace (A412, ASM) to increase the bonding strength. Again, the void formation inspection was performed for all bonded wafers by in-line SAM. The bonded wafers are then subjected to dicing process to prepare 20 × 20 mm^2 die samples. The bonding interface of these diced samples is characterized using TEM (combined with Energy dispersive X-ray (EDS)).

For the PAS measurement, another set of identical bonded wafer pair is prepared. After the wafer bonding and PBA, the top Si was removed on 300 mm wafer level to allow the positron beam to reach the bonding interface. The top Si substrate of the bonded wafer pair was thinned down from 775 μm to approximately 5 μm by using grinding, CMP, and wet etching processes. After the top Si removal step, the bonded wafers were then diced in of 20 × 20 mm^2 samples for PAS measurements. Finally, the residual top Si of the diced samples was completely removed by TMAH rinsing. These samples were then subjected to PAS measurement.

Characterization methodology.—In this study, the inspection of void formation during the PBA for SiO_2 and SiCN film was performed, and the origin investigation was carried out with fundamental characterization techniques followed by standard inspections. Some of the analytical techniques used are not standard techniques for the film characterization of the direct bonding. Therefore, the measurement principle and technical parameters are represented in the following subsections.

Scanning acoustic microscopy.—Firstly, the micro-level void is technically inspected by SAM. SAM is a widely used non-destructive technique to inspect the bonding structure, defect, and interface using acoustic waves. The transducers generate an acoustic wave ranging from 30 MHz to 1 GHz frequency, giving a lateral (x-y) resolution down to 1 μm depending on the transducer and sample material. The propagation property of emitted acoustic waves depends on the mechanical properties of the sample and are also particularly sensitive to material boundaries, e.g., bonding interface. During the measurement, the transducer and target sample are immersed in deionized and degassed water to ensure that the ultrasound waves propagate to and through the samples. The acoustic wave then penetrates the targeted materials through water. The wave is reflected at each interface depending on the reflection coefficient of the interface. If the acoustic wave reaches the interface between silicon and an air gap (unbonded area, void at the bonding interface), the signal is strongly reflected. The SAM system observes the peak of the reflected wave as an echo signal. These echo signals are scanned on the whole target plane and 2D images of the targeted layer are created, so-called C-SAM mode. The image contrast corresponds to the intensity of reflected echo signal, the perfectly bonded area is shown as black area and a void appears as a white spot in 2D image. In this study the in-line automatic SAM with 175 MHz transducer (resolution of 40 μm $pixel^{-1}$) was used for the bonding uniformity inspection of 300 mm bonded wafers. This means that the SAM detection limit using 175 MHz under the full-thickness 775 μm Si substrate is limited for a void with minimum 40 μm in diameter. The bonding uniformity of 300 mm bonded wafer pairs is inspected twice, after the room temperature bonding and after PBA. The void formation inspection using SAM on 300 mm bonded wafer pairs is represented in detail in earlier report.[10]

Positron annihilation spectroscopy.—Based on the macroscopic observation by SAM, the SiO_2 and SiCN film are characterized at atomic scale using PAS. Positron Annihilation Spectroscopy (PAS) is a measurement technique used to evaluate the atomic-level open space in the material. PAS uses positron radiation that annihilates with an electron of the sample resulting in a γ-ray radiation at the same time of its annihilation. The positron is the antiparticle of the electron which has the identical numerical properties such as mass and spin but the opposite charge. When positrons are injected into a solid body, the positron immediately loses the kinetic energy and is thermalized in terms of being in thermal equilibrium in the material. After the thermalization, the positron will interact with the electrons of the material and annihilate rapidly. Two γ-rays are then emitted almost-simultaneously in opposite direction with specific energy range given by:

$$E_\gamma = h\nu \pm \Delta E_\gamma$$

where h is plank constant, ν is the frequency of light, therefore $h\nu =$ 511 keV, $\Delta\ E\gamma$ can be given as:

$$\Delta E_\gamma = p_L c/2$$

where p_L is the electron momentum, c is the velocity of light. The energy distribution of γ-ray that is emitted by positron annihilation shows a Doppler broadening centered on 511 keV due to the momentum component during the positron annihilation. When a positron is injected into an amorphous material, it elastically collides with atoms in material, leading the slowing down and the thermalization of injected positron. During this thermalization, some positrons may react with an electron from molecules in materials and form a bound state, namely positronium, Ps. Ps has two bound states: an anti-parallel spin (para-positronium, p-Ps) state and a parallel spin (ortho-positronium, o-Ps) state. The formation probability of each status of positronium is expected to be 25% for p-Ps and 75% for o-Ps.[11] Constrained by conservation laws, p-Ps annihilates with emitting two γ-rays and o-Ps annihilates with emitting three γ-rays.[12,13] However, the annihilation of o-Ps which the positron in o-Ps annihilates with surrounding electron emitting two γ-rays, so-called pick-off annihilation, is the most probable for annihilation properties of Ps.[12,13] If the positron or Ps diffuse into defect-free material, they mostly meet the orbital electron possessing high momentum, resulting in higher Doppler broadening in the energy distribution of emitted γ-rays. On the other hand, in a material with multiple vacancy defects, injected positron and Ps are localized in the vacancy defect due to Coulomb repulsion from positive ion cores. Consequently, because of reduced possibility of the positron and Ps annihilation with high momentum electrons in the bulk and high possibility of the annihilation with valence electron, the energy distribution of γ-rays emitted from vacancy defect become narrower than that of the annihilation with orbital electron in the defect-free bulk. The energy distribution including Doppler broadening can be characterized by S parameters, defined as the ratio of the number of annihilation events occurring within the energy range of 511 ± 0.76 keV compared to the total annihilation events. Typically, the S parameter remains as the value of around 0.5. The high S parameter indicates the smaller Doppler effects in energy distribution, which means high possibilities of positronium annihilated in open space. On the other hand, a low S parameter can be interpreted such as the tested material has less-vacancy at atomic level.

In addition, the S parameter can be then characterized as the function of the implantation energy of positron. The penetration depth of positron in material can be roughly adjusted by changing the implantation energy of positron. The mean implantation depth of positron was extracted from the incident positron energy by using a prediction technique, described in previous study.[14] However, it must note that the positron travel has the depth profile depending on the implantation energy, meaning it does not exactly reach the single depth. The depth profile becomes broad with higher implantation energy, meaning that the annihilation events with higher implantation energy includes the annihilation event happening at the different depth. Finally, the relationship between parameter S and the implantation energy of positron E was analyzed by VEPFIT, a computer program developed by A. van Veen et al.[15] and then the graph of S-E curve is obtained. In this work, the void formation during Post Bond Anneal (PBA) and thus open space is investigated using PAS and an interpretation of the S parameters for the SiO_2 and SiCN is reported. In this respect the largest open space that PAS can detect is in the order of few nm since the large pore over a few nanometers increase the possibility of self-annihilation of o-Ps emitting three γ-rays, which cannot be analyzed by S parameter. The detailed principle and analysis technique of PAS are presented in other reports.[8,11–14,16]

Electron spin resonance.—The dangling bonds in terms of paramagnetic defects in the deposited film were characterized using Electron Spin Resonance (ESR) for SiO_2 and SiCN in this study. Electron spin resonance is a type of spectroscopy that detects unpaired electrons using Zeeman effect. The detailed principle is presented in the book.[17] The energy gap ΔE induced by Zeeman effect is derived as:

$$\Delta E = h\nu = g\mu_B H$$

where g is a constant value determined by the environment in which the electrons are placed (free electrons, in molecules or ions, etc.), generally referred as g-factor, μ_B is the Bohr magneton, a constant value of 9.274×10^{-24} J T^{-1}, H is magnetic field. When an electromagnetic wave with energy equal to ΔE (the photon energy $h\nu$) is irradiated, the electromagnetic wave is absorbed. ESR detects unpaired electrons by using first derivative of the microwave absorption. The identification of paramagnetic defect is analyzed based on extracted g-factor in ESR spectra since the g-factor is specific to the wave function of the electron. In the earlier studies,[18–20] the dangling bonds formation in SiCO and SiCN film which is aimed to be used as bonding layer, was studied with ESR. It was observed that SiCN films have large amount of silicon and carbon dangling bonds (DBs) after the N_2 plasma activation. However, the correlation between DBs and the bonding chemistry involved at the interface is not explained clearly yet. In this study, the dangling bond formation of SiO_2 and SiCN were evaluated by ESR spectrometer (BRUKER Elexsys E580) at Torey Research Center, Inc. Each sample was cut into 3 pieces with a size of 3×13 mm^2 and the planes of the Si substrate were set perpendicular to the direction of the external magnetic field (Si(100)⊥H). The X-band ESR measurements were performed with 100 kHz modulation frequency (0.2–0.4 mT) by using super-high-Q cavity at 10 K for SiO_2 and 20 K for SiCN sample. Based on the observation of ESR, the impact of dangling bonds on the bonding chemistry of SiO_2 and SiCN is discussed.

Hf area density measurement for the study of OH concentration.—To confirm the direct bonding chemistry, the OH concentration of the surface and the bonding interface structure are studied by $HfCl_4$ ALD deposition. For the direct bonding of Si-based dielectric layer such as SiO_2 and SiCN using plasma surface activation, hydrophilicity of the surface is one factor to be monitored. To quantitatively study the OH concentration on the surface, a method developed earlier was used, based on using an $HfCl_4$ ALD process.[9] The adsorption of the Hf precursor in the initial growth process assumes a direct correlation between the amount of Hf and OH groups on the surface. L. Nyns et al.[9] have introduced the chemical reaction of the ALD of HfO_2 from $HfCl_4$ depending on the amount of OH groups at the exposed surface:

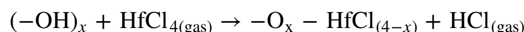

$$(-OH)_x + HfCl_{4(gas)} \rightarrow -O_x - HfCl_{(4-x)} + HCl_{(gas)}$$

where x is the number of OH groups reacting to $HfCl_4$ molecule (x = 1, 2, or 3). $HfCl_4$ molecule reacts with x pieces of OH groups and the oxygen atoms in OH groups combine with Hf in $HfCl_{(4-x)}$. In this case the amount of Hf atoms in $HfCl_{(4-x)}$ is equivalent to the amount of oxygen atoms in OH groups, meaning 1 to 1 amount relation between OH groups and Hf atoms on the surface at first cycle. Therefore. by measuring the density of Hf on the surface by RBS analysis OH concentration can be quantitatively extracted. L. Peng et al.[21] have quantitatively demonstrated the hydrophilicity on the SiCN surface followed by N_2 and Ar-O_2 surface plasma activation by using this technique, showing the explicit increase of hydrophilicity after surface plasma activation. In this study, same characterization technique using the first cycle ALD Hf deposition was performed by using $HfCl_4$ and H_2O as source gas and Rutherford Back-Scattering Spectroscopy (RBS) to measure the Hf concentration on the target surface.

Transmission electron microscopy.—TEM is a standard characterization technique to evaluate the cross-section of the sample at the

nano scale. Typically, the chemical composition analysis can be also extracted using an EDS module in the TEM tool. Also for this study, high angle annular dark field STEM (HAADF-STEM) of the SiO_2 and SiCN bonded sample after the PBA at 250 °C were obtained by TEM (FEI Tecnai F30 ST) at 300 kV and chemical analysis was performed on the corresponding cross-section by EDS analysis. EDS can analyse the chemical composition of silicon, carbon, nitrogen, and oxygen of the cross-section. 50 nm thick lamellas samples for TEM analysis were prepared by focus ion beam.

Results and Discussion

Figure 1 shows the SAM pictures of SiCN and SiO_2 after the PBA at 250 °C and at 350 °C. SiCN wafers did not show any measurable void formation after both PBA processes. This bonding uniformity and thermal stability of SiCN have been demonstrated also in the past study.[22] On the other hand, the SiO_2 wafer pair shows voids formation after a PBA process of 350 °C while it appears void free after 250 °C. A. Castex et al.[22] have demonstrated that the edge void is considered to be the water condensation induced by humid air evacuation at the wafer edge. The void formation after the PBA at 350 °C related the water is discussed in following sections.

Figure 2 shows the S parameter extracted from PAS measurements as a function of implanted positron energy E for (a) 100 nm/100 nm bonded samples after a PBA at 250 °C or 350 °C and (b) 100 nm SiO_2 and SiCN single layers after N_2 plasma activation and after an anneal process of 250 °C or 350 °C. In Fig. 2a it is possible to observe that the SiCN bonded samples are characterized by a higher S value compared to that of SiO_2. Such difference might be attributed to the fact that SiCN has a lower bulk density compared to the one of SiO_2, 1.85 g cm^{-3} and 2.27 g cm^{-3} for SiCN and SiO_2 respectively. The film density was calculated using mass and thickness measurements. The deposited film contains a variety of the size of open space from the atomic-level and nanometer level. On the other hands, the S parameter characterizes the density of atomic-level open space only. Based on these interpretations, it is assumed that the S parameter of SiCN is higher than that of SiO_2 because SiCN potentially contains larger amount of open spaces than SiO_2 at both atomic-level to nanometer level. The SiO_2 bonded sample after the PBA at 350 °C shows a higher S parameter compared to the one which is measured for the sample subjected to the PBA at 250 °C as shown in Fig. 2a. On the other hand, the SiCN bonded sample has no significant change of S parameter between the PBA at 250 °C and 350 °C. This trend is consistent with what is possible to see from the SAM pictures presented in Fig. 1.

As shown in Fig. 2a, the SiO_2 bonded sample subjected to a PBA of 350 °C shows a significant change of S parameter when compared to the one subjected to a PBA of 250 °C. On the contrary the S parameter for SiO_2 100 nm single layer does not show any difference between the anneal at 250 °C and at 350 °C as shown Fig. 2b. This hints to the fact that the increase of S parameter for SiO_2 bonded sample is induced by the bonding process. To be noted here that the open spaces detected by PAS cannot be identified with the bonding voids detected by SAM. The smallest void that SAM can detect is 40 μm. Such size would be too big as open space to be detected by

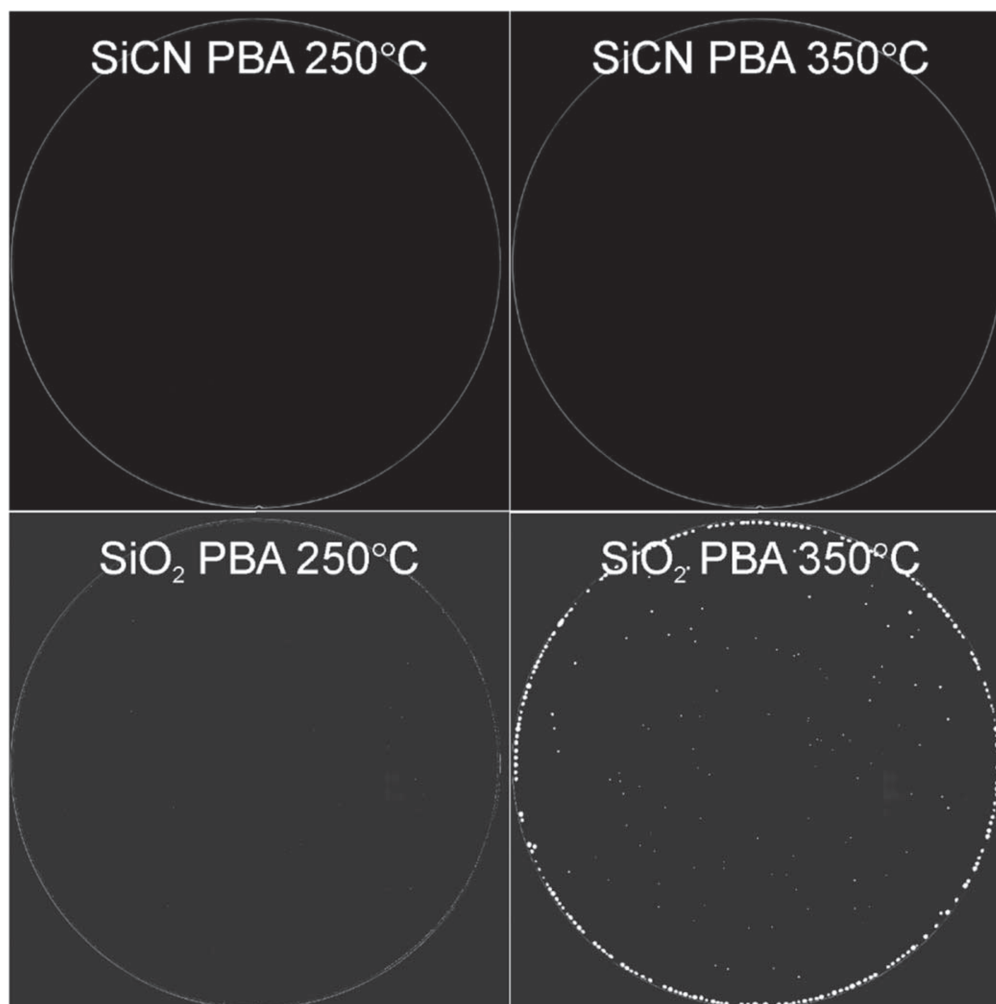

Figure 1. SAM pictures of SiCN and SiO_2 bonded wafer after the PBA at 250 °C and 350 °C.

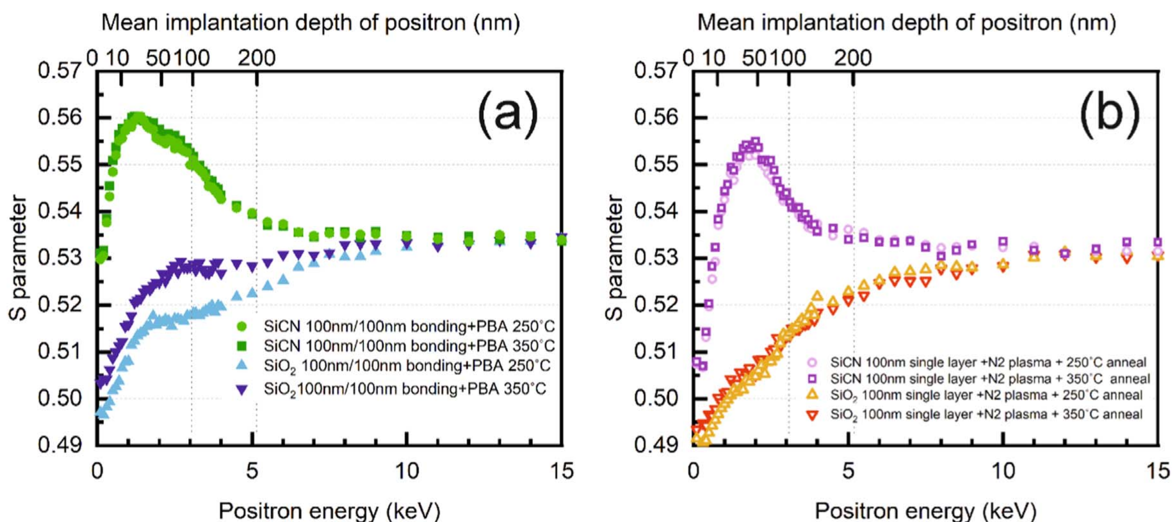

Figure 2. The S parameter as a function of implanted positron energy E of: (a) 100 nm/100 nm bonded pairs and (b) 100 nm single layer for SiCN and SiO_2.

PAS which can detect open spaces in the nm range. In a PAS study performed on CVD SiO_2, M. Sometani et al.[23] have demonstrated that the *S* parameter of SiO_2 film deposited using tetraethoxysilane (TEOS) significantly increased after the annealing at 600 °C due to the desorption of impurities present in the open space. A similar mechanism could be envisioned for the bonded SiO_2 samples: open spaces detected by PAS are created during the annealing process by desorption of molecules such as water. Filled open spaces would form during the surface activation bonding process. These desorbing molecules would in turn form micro voids by clustering at the interface after 350 °C PBA. The same observation is not possible for SiO_2 single layers since in this case we are dealing with an "open system" rather than a closed one and it is expected that the moisture would always be desorbed during the annealing process and immediately re-adsorbed by exposing it again in air.

As shown in Fig. 2a, the SiCN film does not show any creations of open space at the bonding interface between 250 °C and 350 °C PBA. The absence of voids could be explained by the fact that SiCN film possesses the ability not to form open space or voids at interface during the PBA at 350 °C. The further discussion is presented in the latter section.

ESR analysis was performed for the 100 nm SiO_2 and SiCN single layer before and after N_2 plasma to study the impact of dangling bonds in the SiO_2 and SiCN film. Figure 3 shows the ESR spectra on K-band for SiCN samples at 20 K and SiO_2 samples at 10 K before and after N_2 plasma activation. A broad signal was observed characterize by g = 2.003 for each SiCN sample before and after N_2 plasma activation, which is caused by dangling bonds produced in the SiCN film. The DB formation even before the N_2 plasma activation is assigned to the DBs produced during the PECVD process. Based on the spectra configuration and the value of the g-value, it is possibly caused by silicon DBs in Si-N_x and carbon DBs in C-N_x. On the other hand, both SiO_2 samples before and after N_2 plasma activation showed a really weak ESR signal. Figure 4 shows the DB density value per area calculated from the ESR signal. The DB density of SiO_2 sample before N_2 plasma activation showed the lowest DB density value as 2.3×10^{13} cm^{-2}, and after N_2 plasma activation, little increased amount of DB density in the SiO_2 film was observed. As shown in Fig. 4, SiCN film after the N_2 plasma activation shows a large increase of DB density, over 20 times larger than SiO_2 film after N_2 plasma activation. Such large amount of DBs generated after plasma activation in SiCN film was previously observed in past studies.[18–20] Moreover, in the same study an ESR analysis was performed on bonded SiCN samples subjected to a annealing of 250 °C After the room temperature bonding and PBA process at 250 °C, DBs in the SiCN film were greatly consumed as over 60% of total DBs formed by N_2 plasma activation, meaning a significant contribution of DBs at PBA process after the direct bonding. However, lower percentage of DB density was observed in SiO_2 bonded samples.

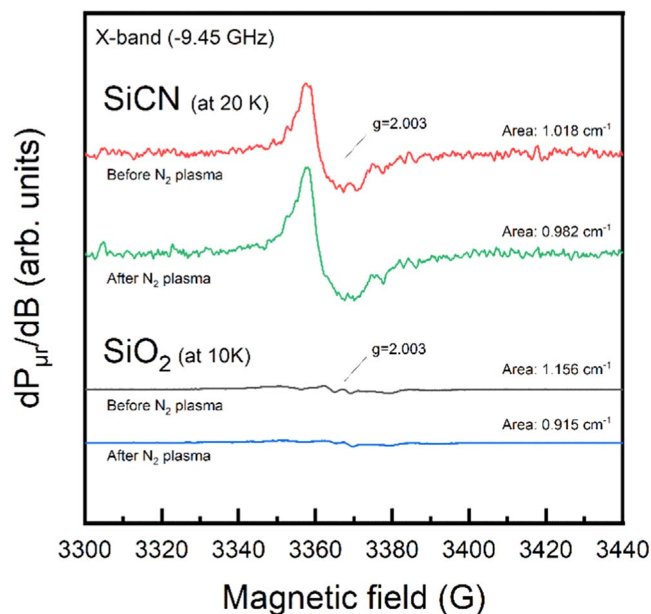

Figure 3. ESR spectra for SiO_2 single layer at 10 K and SiCN single layer at 20 K before and after N_2 plasma activation.

Figure 5 shows HAADF-STEM pictures combined with EDS analysis results for SiCN/SiCN (Fig. 5a) and SiO_2/SiO_2 (Fig. 5b) bonded wafers which were subjected to a 250 °C PBA treatment. In Fig. 5a, the formation of an intermediate layer is observed at the bonding interface of SiCN. By EDS it is assessed that the layer has a SiO_2 nature, and it is assumed that such layer is produced during the bonding mechanism. While the bonding mechanism of SiO_2/SiO_2 direct bonding has been studied in the past with surface plasma treatment creating the additional SiO_2 layer has been explained in past studies.[24–29] First, when the dielectric surface is exposed under the surface activation plasma, the dielectric surface is activated and terminated by OH group. After the two wafers get in contact at the room temperature bonding, Si-OH groups present on the surface connect via hydrogen-bridge bonds trap H_2O molecules at the interface due to the wafer rinsing process in DI water or air

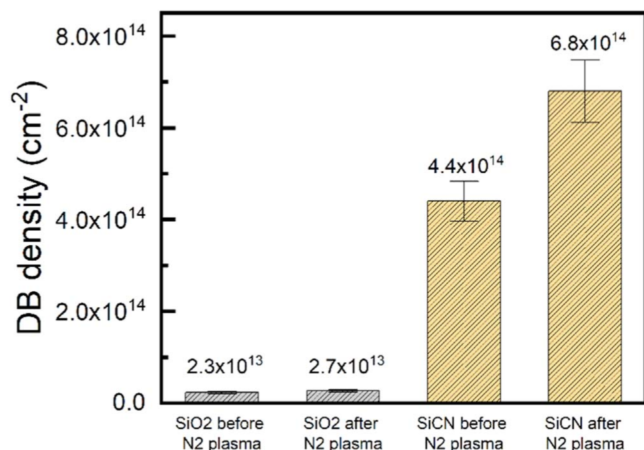

Figure 4. Quantitative value of DB density calculated from the observed ESR signal. The uncertainty is approximately ±10%.

exposure. These sandwiched H_2O molecules migrate or diffuse along the bonding interface to the wafer rim in time. When the Si-OH groups directly meet each other after water molecules diffused away, polymerization of silanol groups starts at a room temperature with forming Si-O-Si bonds and emitting H_2O molecules as by-products, the chemical reaction is derived as:

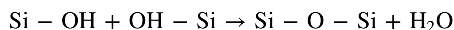

$$\text{Si} - \text{OH} + \text{OH} - \text{Si} \rightarrow \text{Si} - \text{O} - \text{Si} + \text{H}_2\text{O}$$

Based on this condensation reaction, since the SiCN shows the SiO_2-like interface after the PBA 250 °C, SiCN should have a much higher number of Si-OH groups and produce water molecule after the PBA at the interface.

Table II shows the Hf area density value of SiO_2 and SiCN single layer after N_2 plasma activation. A comparable amount of Hf density on the surface was observed between SiO_2 and SiCN films after N_2 plasma activation. This means that the surface of both sample is terminated by OH groups and there is no big difference of OH density between SiO_2 and SiCN layer. Considering the SiO_2 nature of the SiCN-SiCN interface and the fact that after plasma activation the two surfaces have the same hydrophilicity level (similar amount of OH density), it is expected that a similar chemical reaction is happening at the interface of SiO_2-SiO_2 and SiCN-SiCN direct bonding.

Even if the chemical reaction at the interface of SiCN/SiCN is like SiO_2/SiO_2 bonding, the SiCN/SiCN bonding will give rise to void formation. The reason why SiCN is less prone to void formation could be due to the presence of a large amount of DBs. I.G. Batyrev et al.[30] have explained the possible passivation kinetics of silicon dangling bonds (DBs) with water molecule and its favorable passivation reaction path near the SiO_2 interface. The passivation reaction of DBs is described in two paths:

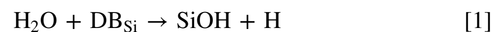

$$\text{H}_2\text{O} + \text{DB}_{\text{Si}} \rightarrow \text{SiOH} + \text{H} \quad [1]$$

or

$$\text{H}_2\text{O} + \text{DB}_{\text{Si}} \rightarrow \text{SiH} + \text{OH} \quad [2]$$

When the silicon DB meets the water molecule, the passivation of DBs happens either with formation of Si-OH bonds and the release of H atoms (reaction 1), which is also reported in other studies,[31,32] or with formation of Si-H bonds and release of OH complexes (reaction 2). The reaction 1 happens with the energy barrier of—0.8 eV and the reaction 2 has an energy barrier of—0.9 eV, which both reactions rarely happen at the room temperature because they need an activation energy. When the SiCN bonded pair receive the PBA process at 250 °C–350 °C, DBs obtain the necessary thermal energy to overcome the energy barrier and then the passivation reaction with water molecule can be initiated. Also, the released OH complex by reaction 2 reacts with remaining DB and passivates it as illustrated in the reaction below:

$$\text{DB}_{\text{Si}} + \text{OH} \rightarrow \text{SiOH} \quad [3]$$

This reaction 3 has an energy barrier of—0.5 eV slightly lower than activation energy of reaction 1 and 2.[30] Moreover, the H atom released by reaction 1 diffuse on the interface and possibly passivate another DB or meet another hydrogen atoms and form hydrogen molecules. It is considered that carbon dangling bonds formed in the

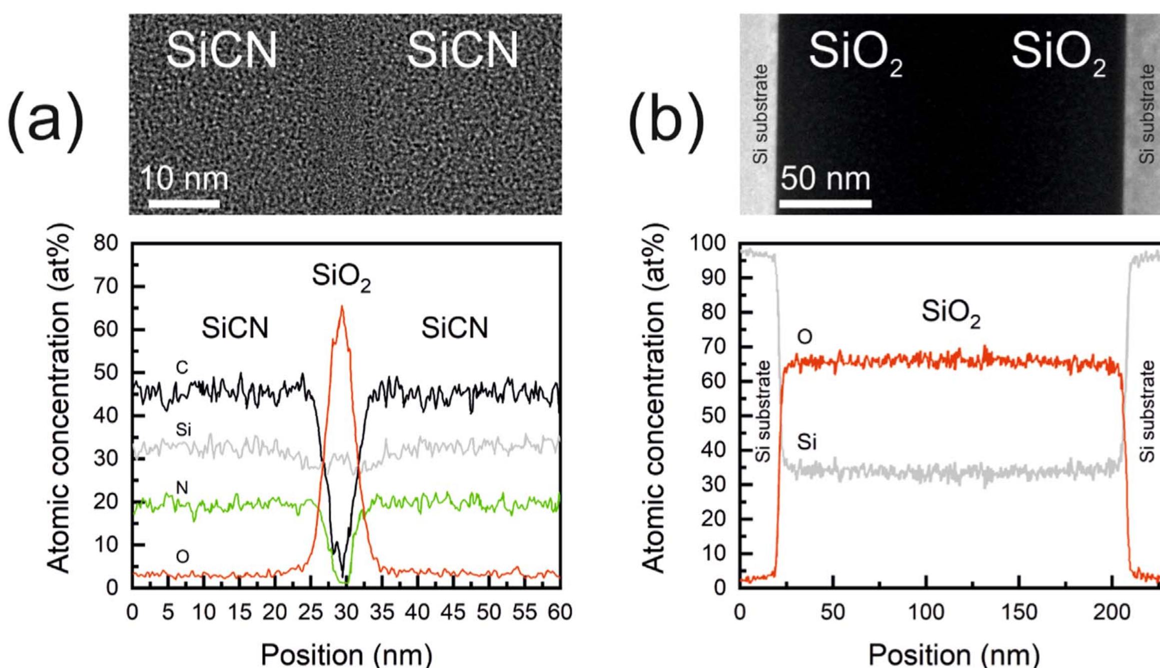

Figure 5. HAADF-STEM pictures and atomic concentration of the cross-section corresponding to the picture for SiCN and SiO_2 bonded sample followed by PBA 250 °C.

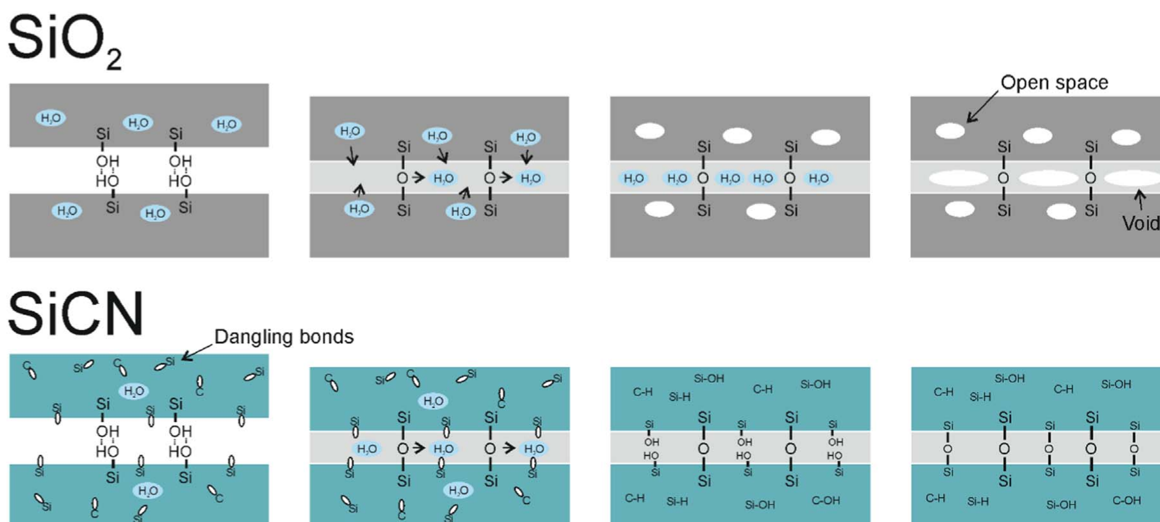

Figure 6. The schematic drawings of model of void formation mechanism for SiO_2 and SiCN.

Table II. Hf area density of SiO_2 and SiCN surface after N_2 plasma activation.

	SiO_2	SiCN
Hf area density, 10^{14} cm^{-2}	2.6 ± 0.1	2.3 ± 0.1

SiCN film are easily passivated by hydrogen atoms diffused around as the passivation of carbon dangling bonds by hydrogen is the major reaction.[33,34] In addition, V. I. Ivashchenko et al.[35] have reported that hydrogen is the most favorable bond of carbon in the hydrated SiCN film. Based on reactions 1, 2, and 3, the model of void formation mechanism related to silicon and carbon DBs for SiO_2 and SiCN was presented in Fig. 6. There are two possible water resources in the bonding system: water molecules absorbed in the film or surface and by-products produced by condensation reaction between Si-OH groups at the interface. For SiO_2, during the PBA at 350 °C the absorbed water in the film evacuates from the surface and empties the open space which can be seen in PAS analysis (Fig. 6a). Simultaneously, the water molecule produced by the condensation reaction evaporates at the interface and appears as a void. Contrary to SiO_2, in the SiCN film, the water molecule reacts with the remaining silicon and carbon DBs in the dielectric film and is captured during the formation of C–H, C–OH, Si–OH or Si–H bonds. This underlying mechanism can explain the absence of any change of *S* parameter of PAS analysis. Moreover, remaining DBs react with the water molecules newly produced at the interface. Especially, the Si–OH newly formed from silicon DB at the surface interacts with that at the opposite surface and Si–O–Si bonds are newly formed in between. This chemical reaction is repeated at the interface of SiCN and water molecules continue to be consumed, resulting in no void formation at the interface during PBA at 350 °C. Therefore, SiCN can suppress the void formation produced by evaporation of absorbed or newly produced water thanks to the work of DBs. In contrast, it can be considered that since SiO_2 layer has minimal DB formation, SiO_2 cannot capture and consume the water molecule in the film and interface. They evaporate during the PBA at 350 °C, resulting in a void at the interface.

Conclusions

The SiO_2 and SiCN bonded samples were investigated by SAM, PAS, and ESR techniques. The presence of void formation on SiO_2 bonded sample was confirmed by SAM, while SiCN bonded sample showed stable bonding without any void formation. By PAS analysis, the creation of open space for SiO_2 bonded wafer pair after the PBA at 350 °C was observed through the increase of *S* parameter from that of PBA at 250 °C. Considering the observation of SAM and PAS, the evacuation of moisture (water molecules) absorbed in the open space is considered as one of origin of void formation. The density of dangling bonds in the SiO_2 and SiCN was evaluated by ESR analysis. Based on the difference of DB density between SiO_2 and SiCN, the void formation mechanism of SiO_2 and SiCN was modelled. The suppression effect of void formation for SiCN were explained by the contribution of chemical reaction between DBs and water molecule. On the other hand, since there is no DBs in SiO_2 film the water molecule stays in the open space and at the interface as it is, resulting in void formation at 350 °C PBA.

Acknowledgments

The authors thank to imec's 3D team for valuable input and discussion, and Toray Research Center for the employment of ESR measurement.

ORCID

F. Nagano https://orcid.org/0000-0001-5315-8694

References

1. E. P. DeBenedictis, M. Badaroglu, A. Chen, T. M. Conte, and P. Gargini, *Computer (Long. Beach. Calif).*, **50**, 69 (2017).
2. H. Seo, H. Park, and S. E. Kim, *Packag. Soc.*, **27**, 17 (2020).
3. A. Jourdain, M. Stucchi, G. Van Der Plas, G. Beyer, and E. Beyne, *Proc. - Electron. Components Technol. Conf.*, **2022**, 1531 (2022).
4. X. X. Zhang and J. P. Raskin, *J. Microelectromech. Syst.*, **14**, 368 (2005).
5. K. H. Lee, S. Bao, D. Kohen, C. C. Huang, K. E. K. Lee, E. Fitzgerald, and C. S. Tan, *2015 IEEE 65th Electronic Components and Technology Conference (ECTC), 2015-July, 560 (2015).*
6. S.-W. Kim, L. Peng, A. Miller, G. Beyer, E. Beyne, and C.-S. Lee, *2015 International 3D Systems Integration Conference (3DIC), TS7.2.1 (2015).*
7. E. Beyne et al., *2017 IEEE International Electron Devices Meeting (IEDM), 32.4.1 (2017).*
8. R. Krause-Rehberg and H. S. Leipner, *Solid-State Sciences* (Berlin, Springer, Berlin) 127 (1999).
9. L. Nyns, A. Delabie, M. Caymax, M. M. Heyns, S. Van Elshocht, C. Vinckier, and S. De Gendt, *ECS Trans.*, **16**, 257 (2008).
10. F. Nagano, S. Iacovo, A. Phommahaxay, F. Inoue, F. Chancerel, H. Naser, G. Beyer, E. Beyne, and S. De, *ECS J. Solid State Sci. Technol.*, **11**, 063012 (2022).
11. M. D. Harpen, *Med. Phys.*, **31**, 57 (2003).
12. F. Tuomisto and I. Makkonen, *Rev. Mod. Phys.*, **85**, 1583 (2013).
13. W. Brandt, S. Berko, and W. W. Walker, *Phys. Rev.*, **120**, 1289 (1960).
14. P. J. Schultz and K. G. Lynn, *Rev. Mod. Phys.*, **60**, 701 (1988).
15. A. van Veen, H. Schut, J. de Vries, R. A. Hakvoort, and M. R. Ijpma, *AIP Conf. Proc.*, **218**, 171 (1991).
16. A. Uedono, S. Ishibashi, K. Tenjinbayashi, T. Tsutsui, K. Nakahara, D. Takamizu, and S. F. Chichibu, *J. Appl. Phys.*, **111**, 014508 (2012).

17. J. E. Wertz and J. R. Bolton, *Electron Spin Resonance: Elementary Theory and Practical Applications* (Netherlands, Springer) (1986).
18. L. Peng et al., *2018 IEEE Int. Interconnect Technol. Conf.*, **179**, 179 (2019).
19. L. Peng, S.-W. Kim, S. Iacovo, J. De Vos, B. Schoenaers, A. Stesmans, V. V. Afanas'ev, A. Miller, G. Beyer, and E. Beyne, *2020 IEEE 22nd Electronics Packaging Technology Conference, EPTC*, **2020**, 464 (2020).
20. F. Inoue, L. Peng, S. Iacovo, F. Nagano, E. Sleeckx, G. Beyer, A. Uedono, and E. Beyne, *2019 6th International Workshop on Low Temperature Bonding for 3D Integration (LTB-3D)*, **732**, 106501 (2019).
21. L. Peng, S.-W. Kim, S. Iacovo, F. Inoue, J. De Vos, E. Sleeckx, A. Miller, G. Beyer, and E. Beyne, "Pre-bonding characterization of SiCN enabled wafer stacking." *6th International Workshop on Low Temperature Bonding for 3D Integration, LTB-3D 2019*, **155**, 14 (2019).
22. A. Castex, M. Broekaart, F. Rieutord, K. Landry, and C. Lagahe-Blanchard, *ECS Solid State Lett.*, **2**, 2 (2013).
23. M. Sometani, R. HaSunuma, M. Ogino, H. Kuribayashi, Y. Sugahara, A. Uedono, and K. Yamabe, *Jpn. J. Appl. Phys.*, **51**, 021101 (2012).
24. R. Stengl, T. Tan, and U. U. Gösele, *Jpn. J. Appl. Phys.*, **28**, 1735 (1989).
25. C. Ventosa, C. Morales, L. Libralesso, F. Fournel, A. M. Papon, D. Lafond, H. Moriceau, J. D. Penot, and F. Rieutord, *Electrochem. Solid-State Lett.*, **12**, 373 (2009).
26. T. Plach, K. Hingerl, S. Tollabimazraehno, G. Hesser, V. Dragoi, and M. Wimplinger, *J. Appl. Phys.*, **113**, 094905 (2013).
27. F. Fournel, C. Martin-Cocher, D. Radisson, V. Larrey, E. Beche, C. Morales, P. A. Delean, F. Rieutord, and H. Moriceau, *ECS J. Solid State Sci. Technol.*, **4**, 124 (2015).
28. C. Sabbione, L. Di Cioccio, L. Vandroux, J. P. Nieto, and F. Rieutord, *J. Appl. Phys.*, **112**, 063501 (2012).
29. T. Fukushima, H. Hashiguchi, H. Yonekura, H. Kino, M. Murugesan, J. C. Bea, K. W. Lee, T. Tanaka, and M. Koyanagi, *Micromachines*, **7**, 1 (2016).
30. I. G. Batyrev, D. M. Fleetwood, R. D. Schrimpf, and S. T. Pantelides, *Proc. Eur. Conf. Radiat. its Eff. Components Syst. RADECS, June 2014 (2007)*.
31. R. E. Stahlbush, R. K. Lawrence, H. L. Hughes, and N. S. Saks, *IEEE Trans. Nucl. Sci.*, **35**, 1192 (1988).
32. M. Pejovic and G. Ristic, *Solid State Electron.*, **41**, 715 (1997).
33. A. Weerasinghe, A. Ramasubramaniam, and D. Maroudas, *Mater. Res. Express*, **5**, 115608 (2018).
34. G. Pennington and C. R. Ashman, *Appl. Phys. Lett.*, **91**, 2 (2007).
35. V. I. Ivashchenko, O. K. Porada, A. O. Kozak, V. S. Manzhara, O. K. Sinelnichenko, L. A. Ivashchenko, and R. V. Shevchenko, *Int. J. Hydrogen Energy*, **47**, 7263 (2022).